Advanced Chemistry Classroom and Laboratory

edited by
Joseph J. BelBruno
Dartmouth College
Hanover, NH 03755

How Mathematics Figures in Chemistry: Some Examples

John Andraos
Department of Chemistry, The University of Queensland, Brisbane, QLD 4072, Australia

During my undergraduate and graduate school studies in physical organic chemistry I have encountered some important chemical problems that are best analyzed using fundamental mathematical concepts. In this article I will discuss four important problems from widely differing areas in physical organic chemistry. Standard texts in spectroscopy (*1*), physical organic chemistry (*2*), and photochemistry (*3*) either do not address these problems or give sketchy details about them. Yet the current literature and general education of chemists demand that somehow we should know the solutions to these problems, if not how the results can be verified. The first two problems are in the areas of mass spectrometry and nuclear magnetic resonance spectroscopy. The third involves potential energy surfaces and the Marcus equation (*4*), and the fourth is in the area of photochemistry, the prediction of the possible multiplicities of products given the multiplicities of reactants. In each case, the problem will be stated and the methodology of solution using some mathematical technique will be presented with illustrative examples where appropriate.

Problem 1. Mass Spectrometry: Use of the Binomial Theorem and Tree Diagrams

In the mass spectra of halogenated compounds it is well known that there are distinctive isotopic patterns for the molecular ion peak, depending on the number and kind of halogenated atoms in the molecule. For example, if a compound contains a single chlorine atom then the molecular ion peak region of the spectrum contains two lines whose intensities are approximately in the ratio 3:1 and which correspond to M and M + 2, respectively. This ratio is determined from the natural abundance of each type of isotope. For chlorine there are two isotopes to consider, ^{35}Cl and ^{37}Cl, in abundances of 75.4% and 24.6%, respectively. The intensity pattern is more complicated when there are multiple chlorine atoms. If there are two chlorine atoms, there are three lines with an intensity ratio of 1:0.653:0.106, corresponding to the M, M + 2, and M + 4 peaks; and if there are three chlorine atoms, there are four lines in the ratio1:0.978:0.319:0.035, corresponding to the M, M + 2, M + 4, and M + 6 peaks. The understanding of how these results are obtained can then be used to predict the ratio of intensities of the molecular ion peaks of a molecule having any number of halogen atoms and also of molecules containing mixed types of halogen atoms of any number. The problem can be extended to include all elements having more than one isotope. More generally, the problem can be stated as:

> Given a molecule containing n_1 atoms of element X_1, n_2 atoms of element X_2, etc. predict the relative intensities of the molecular ion peak pattern for the molecule, given that element X_1 has m_1 isotopes in relative abundance $p_1:p_2:\ldots:p_{m_1}$, element X_2 has m_2 isotopes in relative abundance $q_1:q_2:\ldots:q_{m_2}$, and so on.

Most references will give illustrations of the isotopic pattern distribution but not include any numerical values (*1, 2*). In ref *1* a partial table is given of the percent abundances of molecular ion peaks for molecules containing a variety of combinations of halogen atoms. Also, Beynon (*5*) gives more extensive tables for nuclides commonly encountered in the mass spectra of organic compounds such as chlorine ($^{35}Cl/^{37}Cl$), bromine ($^{79}Br/^{81}Br$), boron ($^{10}B/^{11}B$), sulfur ($^{32}S/^{33}S/^{34}S$), and silicon ($^{28}Si/^{29}Si/^{30}Si$).

Let us consider once again the simplest case of a molecule containing one chlorine atom. Let p be the probability that the chlorine atom has a mass of 35 and q be the probability that the chlorine atom has a mass of 37. We note that these probabilities are directly related to the percent natural abundances of these isotopes and that the condition

$$p + q = 1 \tag{1}$$

is satisfied. Then, it is obvious that the intensity ratio of the observed two lines will be p:q or 3:1 with p = .754 and q = .246 for the M and M + 2 peaks, respectively. For a compound containing two chlorine atoms we have three lines with a ratio of intensities equal to $p^2:2pq:q^2$, where p^2 is the probability that the molecule contains two ^{35}Cl atoms, $2pq$ is the probability that it contains one ^{35}Cl atom and one ^{37}Cl atom, and q^2 is the probability that it contains two ^{37}Cl atoms. This can be verified by expanding $(p + q)^2$

$$(p + q)^2 = p^2 + 2pq + q^2 = 1 \tag{2}$$

or using the tree diagram shown below.

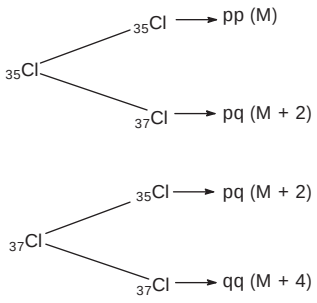

For a compound containing n chlorine atoms the intensity ratio is given by the expansion of $(p + q)^n$,

$$(p+q)^n = \binom{n}{0}p^n + \binom{n}{1}p^{n-1}q + \binom{n}{2}p^{n-2}q^2 + \ldots + \binom{n}{n}q^n = \sum_{j=0}^{n}\frac{n!}{(n-j)!j!}p^{n-j}q^j \tag{3}$$

where we have n + 1 lines corresponding to the M, M + 2, M + 4, etc. peaks. This is just the statement of the binomial

theorem (*6*) and generally the general term in the binomial expansion,

$$\frac{n!}{(n-j)!j!}p^{n-j}q^{j}$$

corresponds to the probability that the compound contains $n-j$ ^{35}Cl atoms and j ^{37}Cl atoms. Furthermore, the percent abundances of the molecular ion peaks relative to the parent M peak of lightest mass is given by

$$\frac{n!}{(n-j)!j!}\left(\frac{q}{p}\right)^{j}\times 100$$

where j = 0, 1, 2, ..., n. Table 1 shows a summary of these relative percent abundances for various numbers of chlorine atoms in a molecule. The same analysis applied to any number of bromine atoms having the isotopes ^{79}Br and ^{81}Br with p = .505 and q = .495 gives the results shown in Table 2. The predictions of the molecular peak distributions based on the abundances of the isotopes of the elements can be verified with experiment. Figure 1 shows the experimental mass spectral molecular ion patterns of hexachlorobenzene and 1,3,5-tribromobenzene compared with their respective predicted patterns.

Now, we consider the case of a molecule containing mixed halogen atoms. The prediction of the isotopic distribution of the molecular ion peaks is more complicated and is best analyzed using tree diagrams. For example, if a molecule has one Cl atom and one Br atom, using the abundances of the relevant isotopes (p_1 = .754 for ^{35}Cl, q_1 = .246 for ^{37}Cl, p_2 = .505 for ^{79}Br, and q_2 = .495 for ^{81}Br) the tree diagram shown below applies.

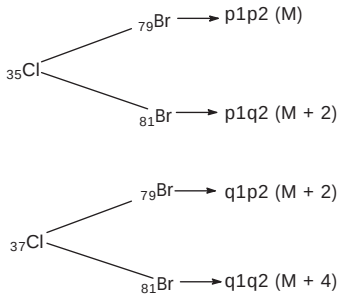

From this we observe that the probabilities corresponding to the M, M + 2, and M + 4 peaks are p_1p_2, $p_1q_2 + q_1p_2$, and q_1q_2, respectively. For a molecule containing two Br atoms and one Cl atom the tree diagram shown below applies and we have

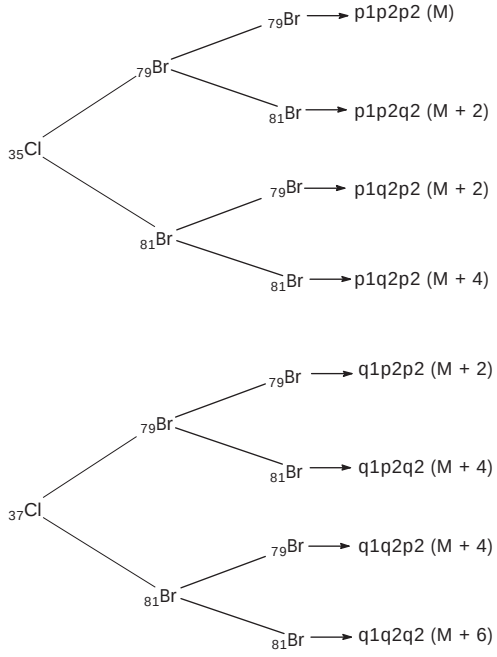

$$\begin{aligned} \mathrm{M} &\Rightarrow p_1(p_2)^2 \\ \mathrm{M}+2 &\Rightarrow (p_2)^2q_1 + 2p_1p_2q_2 \\ \mathrm{M}+4 &\Rightarrow p_1(q_2)^2 + 2q_1p_2q_2 \\ \mathrm{M}+6 &\Rightarrow q_1(q_2)^2 \end{aligned} \qquad (4)$$

Table 3 summarizes the percent abundances for the M, M + 2, etc. peaks for molecules containing various combinations of Cl and Br atoms and Figure 2 compares the mass spectral molecular ion pattern of α-bromo-2,6-dichlorotoluene with the predicted pattern.

The final case considered here pertains to elements having more than two isotopes. An example of this is sulfur, which has three isotopes, ^{32}S, ^{33}S, and ^{34}S, with the corresponding abundances p = .9503, q = .0076, and r = .042.Once again, for a molecule containing one sulfur atom the intensity ratio of molecular ion peaks is p:q:r. For molecules containing more than one sulfur

Table 1. Probabiliy of Occurrence of Peak at Mass M, M + 2, M + 4, ... in Spectra of Molecules with Various Numbers of Chlorine Atoms

Atoms	M	M + 2	M + 4	M + 6	M + 8	M + 10	M + 12	M + 14	M + 16
Cl	.7540	.2460							
Cl_2	.5685	.3710	.0605						
Cl_3	.4287	.4196	.1369	.0149					
Cl_4	.3232	.4218	.2064	.0449	.0037				
Cl_5	.2437	.3976	.2594	.0846	.0138	.0009			
Cl_6	.1838	.3597	.2934	.1276	.0312	.0041	.0002		
Cl_7	.1386	.3164	.3097	.1684	.0549	.0108	.0012	.0001	
Cl_8	.1045	.2727	.3114	.2032	.0829	.0216	.0035	.0003	.0000

NOTE: M is the mass corresponding to molecules containing only ^{35}Cl atoms. More extensive compilations may be found in ref *5*.

Table 2. Probabiliy of Occurrence of Peak at Mass M, M + 2, M + 4, ... in Spectra of Molecules with Various Numbers of Bromine Atoms

Atoms	M	M + 2	M + 4	M + 6	M + 8	M + 10	M + 12	M + 14	M + 16
Br	.5057	.4943							
Br_2	.2557	.4999	.2443						
Br_3	.1293	.3792	.3707	.1208					
Br_4	.0654	.2557	.3749	.2443	.0597				
Br_5	.0331	.1616	.3160	.3089	.1510	.0295			
Br_6	.0167	.0981	.2397	.3124	.2290	.0895	.0146		
Br_7	.0085	.0579	.1697	.2765	.2702	.1585	.0516	.0072	
Br_8	.0043	.0335	.1144	.2237	.2733	.2137	.1044	.0292	.0036

NOTE: M is the mass corresponding to molecules containing only ^{79}Br atoms. More extensive compilations may be found in ref *5*.

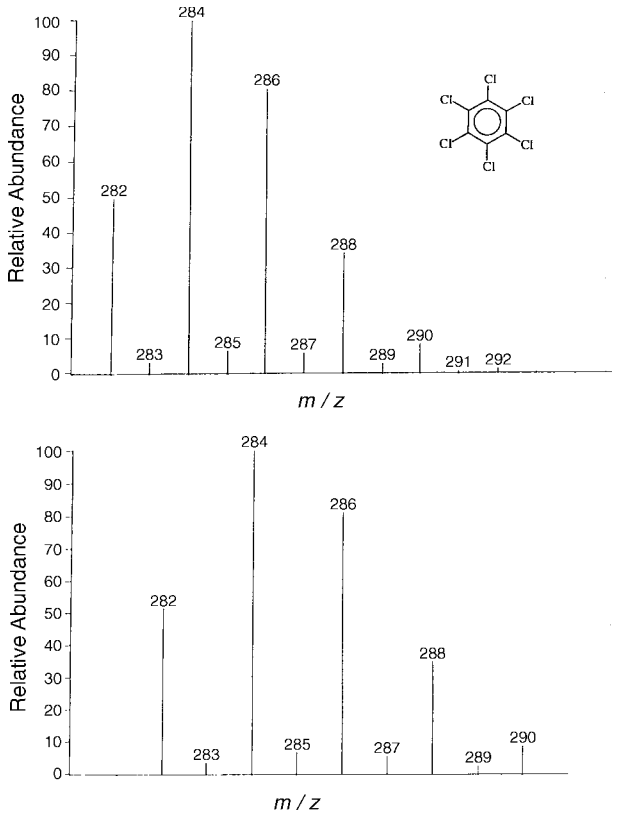

Figure 1a. Partial mass spectrum of hexachlorobenzene showing the experimentally observed molecular ion patterns (top) compared with the corresponding predicted patterns based on the binomial expansion treatment (bottom). The intervening lines of low intensity correspond to molecular ion peaks containing the ^{13}C isotope.

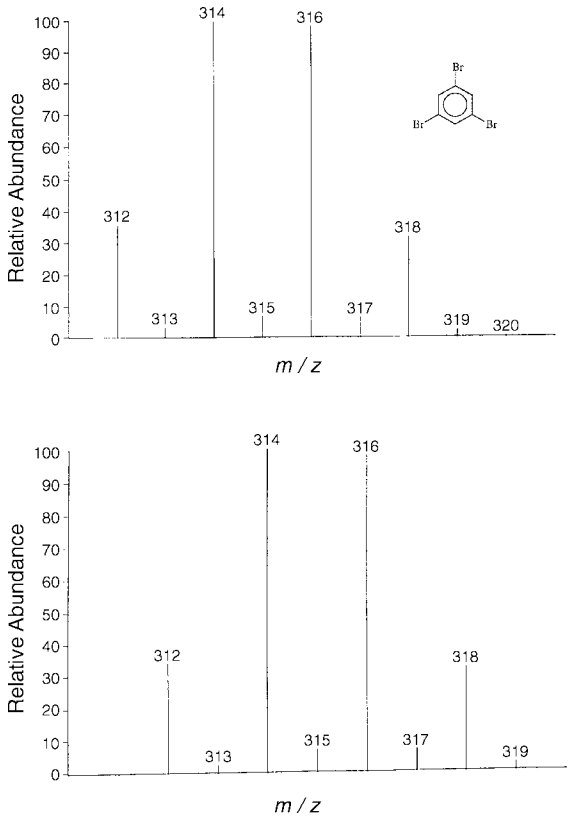

Figure 1b. Partial mass spectrum of 1,3,5-tribromobenzene showing the experimentally observed molecular ion patterns (top) compared with the corresponding predicted patterns based on the binomial expansion treatment (bottom). The intervening lines of low intensity correspond to molecular ion peaks containing the ^{13}C isotope.

Table 3. Probabiliy of Occurrence of Peak at Mass M, M + 2, M + 4, ... in Spectra of Molecules with Various Numbers of Chlorine and Bromine Atoms

Atoms	M	M + 2	M + 4	M + 6	M + 8	M + 10	M + 12	M + 14	M+16
ClBr	.3818	.4971	.1216						
$ClBr_2$	.1928	.4399	.3072	.0601					
$ClBr_3$	.0975	.3177	.3728	.1823	.0297				
Cl_2Br	.2875	.4686	.2140	.0299					
Cl_2Br_2	.1454	.3791	.3398	.1209	.0148				
Cl_2Br_3	.0736	.2636	.3592	.2291	.0672	.0073			
Cl_3Br	.2168	.4241	.2766	.0752	.0074				
Cl_3Br_2	.1096	.3216	.3495	.1728	.0409	.0036			
Cl_3Br_3	.0554	.2168	.3357	.2611	.1071	.0221	.0018		
Cl_4Br	.1634	.3731	.3129	.1247	.0240	.0018			
Cl_4Br_2	.0827	.2964	.3426	.2177	.0738	.0128	.0009		
Cl_4Br_3	.0418	.1771	.3065	.2795	.1450	.0430	.0068	.0004	
Cl_5Br	.1232	.3215	.3277	.1710	.0488	.0073	.0004		
Cl_5Br_2	.0623	.2235	.3246	.2485	.1092	.0278	.0038	.0002	
Cl_5Br_3	.0315	.1438	.2746	.2861	.1780	.0681	.0157	.0020	.0001
Cl_6Br	.0929	.2727	.3262	.2096	.0789	.0175	.0021	.0001	
Cl_6Br_2	.0470	.1829	.2998	.2672	.1435	.0478	.0097	.0011	.0001

NOTE: M is the mass corresponding to molecules containing only ^{35}Cl and ^{79}Br atoms. More extensive compilations may be found in ref *5*.

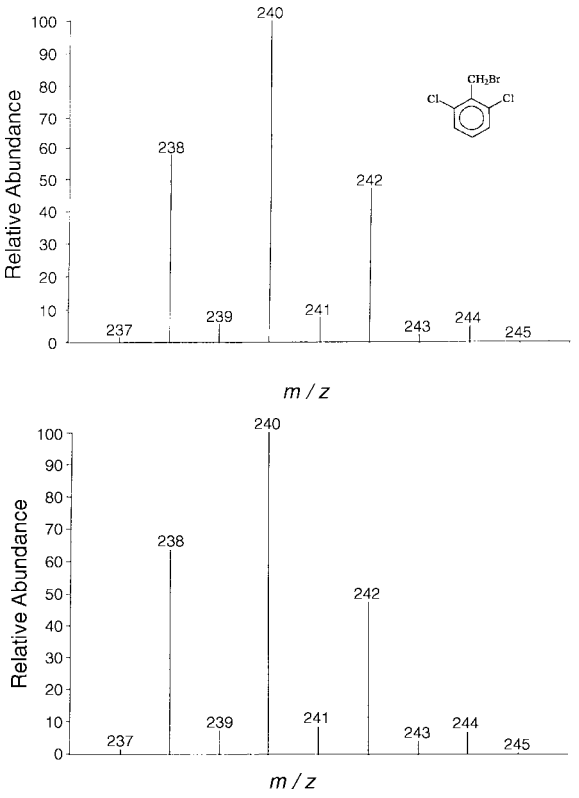

Figure 2. Partial mass spectrum of α-bromo-2,6-dichlorotoluene showing the experimentally observed molecular ion pattern (top) compared with the predicted pattern based on the tree diagram treatment (bottom). The intervening lines of low intensity correspond to molecular ion peaks containing the ^{13}C isotope.

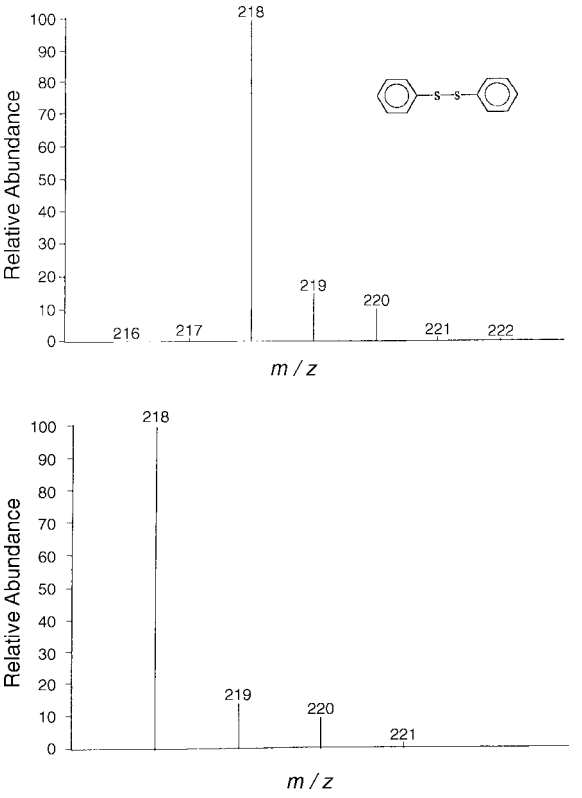

Figure 3. Partial mass spectrum of diphenyldisulfide showing the experimentally observed molecular ion pattern (top) compared with the predicted pattern based on the binomial treatment (bottom).

atom, the binomial expansion is used to predict the molecular ion isotopic pattern. For two sulfur atoms, we have

$$(p + q + r)^2 = p^2 + 2pq + 2pr + q^2 + 2qr + r^2 = 1 \quad (5)$$

and the corresponding probabilities for the molecular ion peak

$$\begin{aligned} M &\Rightarrow p^2 \\ M + 1 &\Rightarrow 2pq \\ M + 2 &\Rightarrow 2pr + q^2 \\ M + 3 &\Rightarrow 2qr \\ M + 4 &\Rightarrow r^2 \end{aligned} \quad (6)$$

Table 4. Probabiliy of Occurrence of Peak at Mass M, M + 1, M + 2, ... in Spectra of Molecules with Various Numbers of Sulfur Atoms

Atoms	M	M + 1	M + 2	M + 3	M + 4	M + 5	M + 6	M + 7	M + 8
S	.9503	.0076	.0420		.0001				
S_2	.9030	.0144	.0799	.0006	.0020				
S_3	.8581	.0206	.1139	.0018	.0054		.0001		
S_4	.8154	.0261	.1445	.0035	.0101	.0002	.0004		
S_5	.7748	.0310	.1717	.0055	.0158	.0004	.0008		
S_6	.7363	.0353	.1960	.0078	.0224	.0007	.0014		.0001
S_7	.6997	.0392	.2174	.0104	.0296	.0012	.0023	.0001	.0001
S_8	.6649	.0425	.2363	.0132	.0375	.0018	.0035	.0001	.0002

NOTE: M is the mass corresponding to molecules containing only ^{32}S atoms. More extensive compilations may be found in ref *5*.

Hence, the corresponding intensity ratio for the 5 peaks is .9030: .0144: .0799: .0006: .0020. Generally, for a molecule containing *n* sulfur atoms we have

$$(p + q + r)^n = \sum_{j=0}^{n} \frac{n!}{(n-j)!j!} \frac{r^j}{(p+q)^j} (p+q)^n \quad (7)$$

where $(p + q)^n$ is evaluated from eq 3. Table 4 summarizes the molecular ion peak isotopic distribution for molecules containing various numbers of sulfur atoms. As an example, Figure 3 shows the mass spectral molecular ion pattern of diphenyldisulfide compared with the predicted pattern.

To answer the problem posed, we can conclude that in general, for a molecule containing n_1 atoms of element X_1 with m_1 isotopes of relative abundance $p_1:p_2:\ldots:p_{m_1}$, n_2 atoms of element X_2 with m_2 isotopes of relative abundance $q_1:q_2:\ldots:q_{m_2}$, etc., the intensities of the molecular ion peaks relative to the parent peak are found from the binomial expansion of

$$\frac{\left(p_1 + p_2 + \ldots + p_{m_1}\right)^{n_1}\left(q_1 + q_2 + \ldots + q_{m_2}\right)^{n_2}}{p_1^{n_1} q_1^{n_2}}$$

where p_1, q_1, etc. correspond to the probabilities of occurrence of the lightest masses of elements X_1, X_2, etc.

Problem 2. NMR Spectroscopy: Integration

When recording the ^{1}H NMR spectrum of a compound it is common practice to integrate the resonance peaks in order to determine the relative number of protons corresponding to a functional group. Chemists take it for granted that the height of the sigmoidal curve drawn above the resonance peak represents the area under it. The problem can be simply stated as

> Prove that the sigmoidal curve drawn above a resonance NMR signal is in fact its integrand function and show that the height of such a curve is identical in magnitude to the area under the resonance signal.

The line shape of an NMR resonance signal is a Lorentzian (*7*) having the form

$$f(\nu) = \frac{2T_2}{1 + 4\pi^2 T_2^{\,2}(\nu - \nu_0)^2} \tag{8}$$

where $f(\nu)$ is the intensity, ν is the frequency in Hz, T_2 is the transverse or spin–spin relaxation time, in seconds, and ν_0 is the resonance frequency in Hz. Applying some basic calculus techniques to the function reveals that it is concave down with the following characteristics:

$$\lim_{\nu \to \infty} f(\nu) = \lim_{\nu \to -\infty} f(\nu) = 0 \tag{9a}$$

$$f(\nu)|_{\max} = 2T_2 \text{ and occurs at } \nu = \nu_0 \tag{9b}$$

$$\text{points of inflection occur at } \nu = \nu_0 \pm \frac{1}{2\sqrt{3}\pi T_2} \tag{9c}$$

Integrating this function over the frequency domain yields

$$F(\nu) = \int f(\nu)\,d\nu = \frac{1}{\pi}\arctan\left(2\pi T_2(\nu - \nu_0)\right) \tag{10}$$

Figure 4 shows the shapes of the functions $f(\nu)$ and $F(\nu)$. The integrand function has the familiar sigmoidal shape. Furthermore, the limiting values of $F(\nu)$ are

$$\lim_{\nu \to \infty} F(\nu) = \frac{1}{2}$$
$$\lim_{\nu \to -\infty} F(\nu) = -\frac{1}{2} \tag{11}$$

and the difference between the limits, corresponding to the height of the curve, is then 1. Evaluating the definite integral of $f(\nu)$ over the full frequency range (the area under $f(\nu)$), leads to the same result:

$$\int_{-\infty}^{\infty} f(\nu)\,d\nu = \frac{1}{\pi}\arctan\left(2\pi T_2(\nu - \nu_0)\right)\Big|_{-\infty}^{\infty} = 1 \tag{12}$$

It should be noted that eq 8 refers to a single nucleus with an associated chemical environment designated by the specific resonance frequency ν_0. For N chemically equivalent nuclei $f(\nu)$ is multiplied by the factor N and hence the area of the Lorentzian is N. It is now clear that the ratio of peak areas in a decoupled NMR spectrum corresponds directly to the ratio of chemically different nuclei in a molecule.

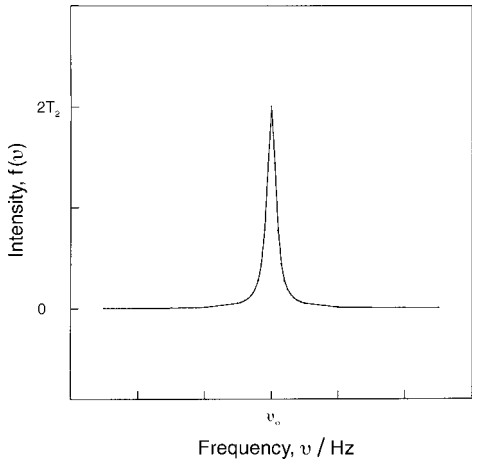

Figure 4a. Graph of the Lorentzian function $f(\nu)$ corresponding to the lineshape of an NMR signal.

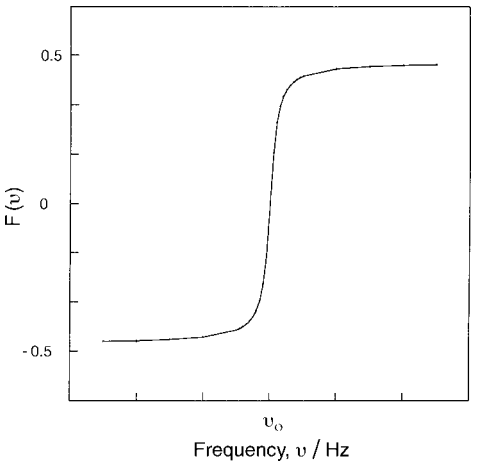

Figure 4b. Graph of the integral of the Lorenztian function, $F(\nu)$.

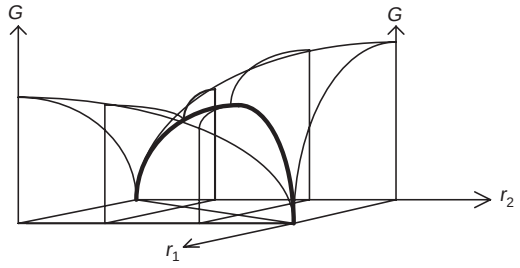

Figure 5. 3-D representation of a reaction surface G as a function of two reaction coordinates, r_1 and r_2. Two-dimensional reaction profiles at fixed r_2 coordinates are depicted as slices along the r_1 axis. The trajectory marked with a thick line corresponds to the reaction profile along the vector sum of the r_1 and r_2 coordinates (adapted from ref *10*).

Problem 3. Marcus Equation: Analytical Geometry and Calculus

When describing the mechanism of a chemical reaction, physical organic chemists resort to potential energy surfaces and potential energy profiles. A reaction mechanism consists of a series of elementary reactions, which can each be represented by a potential energy surface, *S*. *S* is a multidimensional function of at least three variables; one axis represents energy and the other axes represent some geometric parameters relevant to the progress of the reaction (reaction coordinates), such as bond length, bond angle, and torsional (dihedral) angle. The equation of the surface can be written generally as

$$G = G(\ell_1,\ell_2,\ldots,\ell_n,\theta_1,\theta_2,\ldots.\theta_n,\phi_1,\phi_2,\ldots,\phi_l) \qquad (13)$$

where G represents the Gibbs free energy, and ℓ_i, θ_i, and ϕ_i are the ith bond length, bond angle, and dihedral angle, respectively, in the reacting molecule(s). In the vicinity of the minima representing reactant and product states, the surface is approximated by a quadratic function. Of the series of elementary reactions the rate-determining step and its corresponding potential energy surface are the most important. The trajectory along this surface describes the pathway along some reaction coordinates from reactants (initial state) to products (final state) that passes through a transition state for the rate-determining step. The reaction coordinate for this step is a small subset of the geometric parameters given in eq 13; usually no more than two parameters are considered. This consequently facilitates a pictorial representation in 3 or 2 dimensions of the function G. If G is a function of two geometric parameters, then it represents a surface (3-D); if G is a function of one geometric parameter, then it represents a potential energy profile (2-D). In effect, a potential energy profile is a slice taken of the multidimensional surface G along some reaction coordinate (see Fig. 5). Furthermore, in a two-dimensional energy profile the same quadratic approximation is applied to the reactant and product states and leads to the intersecting parabola model to describe the two-dimensional reaction pathway.

The Marcus equation (*4*), applied to electron and proton transfer reactions, relates the change in free energy of activation for the rate determining electron or proton transfer step, $\Delta G^{\#}$, given by

$$\Delta G^{\#} = G^{\#} - G^{\mathrm{IS}} \qquad (14)$$

to the change in free energy of reaction, ΔG°,

$$\Delta G^{\circ} = G^{\mathrm{FS}} - G^{\mathrm{IS}} \qquad (15)$$

through the quadratic function

$$\Delta G^{\#} = \frac{\lambda}{4}\left(\frac{\Delta G^{\circ}}{\lambda} + 1\right)^2 \qquad (16)$$

where G^{IS} and G^{FS} represent the free energies of reactants (initial state) and of products (final state), $G^{\#}$ represents the free energy of the transition state, and λ is related to the intrinsic barrier, $\Delta G_o^{\#}$ ($\lambda = 4\Delta G_o^{\#}$). This relationship links thermodynamic free energies with kinetic free energies and is the crux of simple Marcus rate theory. The problem is stated below.

Part I. Derive the Marcus equation using the intersecting parabola (or oscillator) model.

Part II. Fully characterize the Marcus equation with respect to exoergonic, thermoneutral, and endoergonic electron or proton transfer reactions.

To answer part I we begin by stating that a potential energy profile in two dimensions is approximately described by a parabolic function given in general form

$$(r - p)^2 = 4a(G - q) \qquad (17)$$

where r represents the reaction coordinate (one geometric parameter) and G is the free energy. The minimum point on the parabola is given by the coordinates (p, q); a is positive-valued and gives a measure of the degree of curvature of the parabola. For a values between 0 and 1 the parabola is characterized as having a shallow potential well, whereas for a values larger than 1 it is characterized as having a deep potential well. The fact that a is positive-valued means that the parabola is concave up and the axis of symmetry is parallel to the G axis. Taking two general parabolas

$$\begin{aligned}(r - p_1)^2 &= 4a_1(G_1 - q_1)\\ (r - p_2)^2 &= 4a_2(G_2 - q_2)\end{aligned} \qquad (18)$$

where (p_1, q_1) and (p_2, q_2) represent the coordinates of the reactant (initial) and product (final) states, respectively, we are required to find the intersection point (r_i, G_i) representing the coordinates of the transition state on the energy profile; that is, at what value of r does $G_1 = G_2$. In simple Marcus theory it is assumed that the curvatures of both parabolas is the same ($a_1 = a_2 = a$) and that the horizontal displacement, $p_2 - p_1$, is constant (*4c*). Applying these conditions to eq 18 leads to

$$G_i = \frac{1}{4a}\left(\frac{p_2^2 - p_1^2 + 4a\left(q_2 - q_1\right)}{2\left(p_2 - p_1\right)} - p_1\right)^2 + q_1 \qquad (19)$$

at $r = r_i$ which can be rewritten as

$$G_i = \frac{1}{4a}\left(\frac{\left(p_2 - p_1\right)^2 + 4a\left(q_2 - q_1\right)}{2\left(p_2 - p_1\right)}\right)^2 + q_1 \qquad (20)$$

The change in free energy of activation, $\Delta G^{\#}$, is given by the vertical distance between the point (r_i, G_i) representing the transition state and the point (p_1, q_1) representing the reactant (initial) state (see Fig. 6). Hence,

$$\Delta G^{\#} = G_i - q_1 \qquad (21)$$

or

$$\Delta G^{\#} = \frac{1}{4a}\left(\frac{\left(p_2 - p_1\right)^2 + 4a\left(q_2 - q_1\right)}{2\left(p_2 - p_1\right)}\right)^2 = \frac{1}{4}\left(\frac{4a^2\left(q_2 - q_1\right)^2}{\left(p_2 - p_1\right)^2} + 2\left(q_2 - q_1\right) + \frac{\left(p_2 - p_1\right)^2}{4a^2}\right) \qquad (22)$$

by substituting eq 20 into eq 21. Now, setting

$$\lambda = \frac{\left(p_2 - p_1\right)^2}{4a^2}$$

$$\Delta G^\circ = q_2 - q_1 \qquad (23)$$

where ΔG° is the change in free energy of reaction, and then making these substitutions into eq 22 gives

$$\Delta G^{\#} = \frac{1}{4}\left(\frac{\left(\Delta G^\circ\right)^2}{\lambda} + 2\Delta G^\circ + \lambda\right) \qquad (24)$$

which can be factored to yield the simple Marcus expression in standard form (eq 16). A more complicated expression for $\Delta G^{\#}$ is obtained if the two parabolas have different curvatures (see Appendix).

The characterization of eq 16 involves taking the first and second derivatives of the quadratic function. We find that this is a concave up parabola with a minimum at $(-\lambda, 0)$ (see Fig. 7a). The Marcus equation can also be expressed in terms of the Brønsted α,

$$\Delta G^{\#} = \lambda\alpha^2 = 4\alpha^2\Delta G_o^{\#} \qquad (25)$$

where

$$\alpha = \frac{\partial\left(\Delta G^{\#}\right)}{\partial\Delta G^\circ} = \frac{1}{2}\left(1 + \frac{\Delta G^\circ}{\lambda}\right) = \frac{1}{2}\left(1 + \frac{\Delta G^\circ}{4\Delta G_o^{\#}}\right) \qquad (26)$$

Equation 25 is also a concave up parabola with a minimum at (0, 0) (see Fig. 7b). We note that the intrinsic barrier is always positive-valued and that the free energy of reaction can either be positive- or negative-valued. From Figure 7 we can designate different domains of the parabolic function along the ΔG° axis corresponding to different types of reactions. The three domains given below correspond to conditions for endoergonic, thermoneutral, and exoergonic reactions. These are represented pictorially in Figure 7.

$\Delta G^\circ > 0, \Delta G^{\#} > \Delta G_o^{\#} \Rightarrow$ endoergonic reaction

$\Delta G^\circ = 0, \Delta G^{\#} = \Delta G_o^{\#} \Rightarrow$ thermoneutral reaction

$$\Delta G^\circ < 0, \left\{\begin{array}{c} 0 < \Delta G^{\#} < \Delta G_o^{\#}, \text{ for } -\lambda < \Delta G^\circ < 0 \\ \Delta G^{\#} > 0, \quad \text{for } \Delta G^\circ < -\lambda \end{array}\right\} \Rightarrow$$

exoergonic reaction

For an endoergonic reaction, the transition state is closer in energy to that of the product; therefore, by the Hammond postulate, it is closer in structure to it as well, and is termed a "late" transition state with corresponding α values greater than 1/2. From the figure we observe that as the reaction increases in endoergonicity the free energy of activation also increases, which translates into a decrease in reaction rate. For a thermoneutral reaction, the transition state is halfway in structure between the reactant and product states ($\alpha = 1/2$) and is consequently equidistant in energy between these two states. Again from the figure, the condition of thermoneutrality is represented by a single point $(0, \Delta G_o^{\#})$. For an

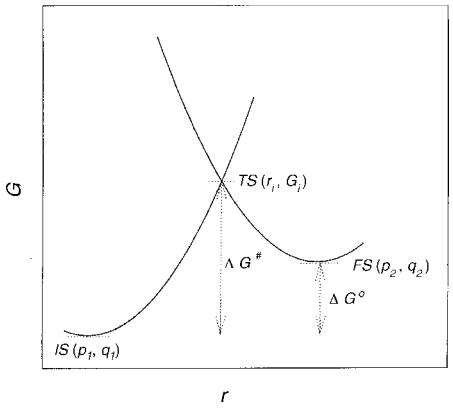

Figure 6. Intersecting parabola model applied to a potential energy profile. The coordinates for the initial (reactant), transition, and final (product) states are shown.

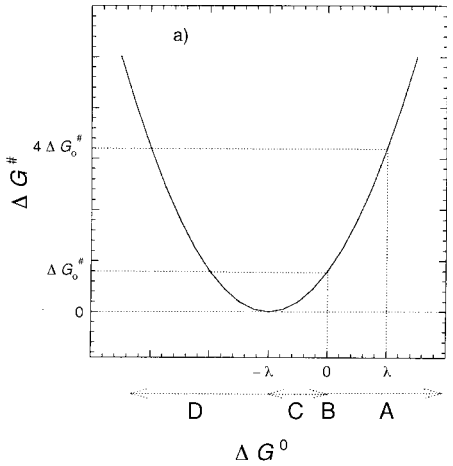

Figure 7a. Plot of $\Delta G^{\#}$ versus ΔG° (eqs 16 and 24) showing endoergonic (region A), thermoneutral (point B), exoergonic with increasing reaction rate (region C), and exoergonic with decreasing reaction rate, "inverted region" (region D) domains.

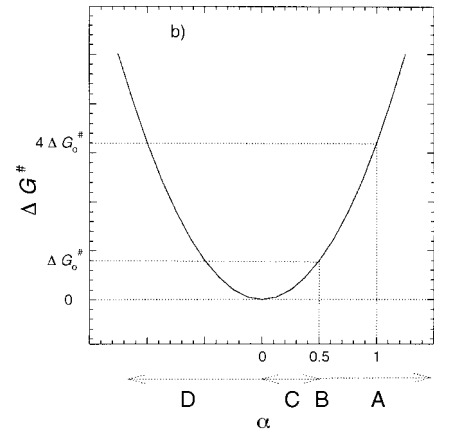

Figure 7b. Plot of $\Delta G^{\#}$ versus α (eq 25) showing endoergonic (region A), thermoneutral (point B), exoergonic with increasing reaction rate (region C), and exoergonic with decreasing reaction rate, "inverted region" (region D) domains.

exoergonic reaction, the transition state structure is closer in energy to the reactant. Once again by the Hammond postulate it is closer to it in structure as well, and is termed an "early" transition state, with corresponding α values less than 1/2. From the figure we observe two subdomains. The first, $-\lambda < \Delta G^\circ < 0$, follows our intuition in that as the free energy of activation decreases the corresponding reaction rate increases. However, this continues until $\Delta G_o = -\lambda$; beyond this point (the minimum in the parabola) the reaction rate no longer increases with increasing exoergonicity. Indeed, the Marcus equation predicts that there should be an "inversion" in reaction rates in this domain, and this was first verified by experiment in solution-phase reactions in 1986 (*8*). The value of this analysis using the intersecting parabola model is that it clearly illustrates this so-called "inverted region".

Problem 4. Photochemistry: Probability

The problem can be stated as:

Given two species, A and B, of known multiplicity, what are the possible allowed multiplicities of the product, C, of the reaction A + B → C, assuming a first encounter between A and B?

For example, if A and B are triplets, what are the possible allowed multiplicities of C? The answer is that C can have 9 possible spin states, with the following probabilities: 5/9 quintet, 1/3 triplet, and 1/9 singlet. How does one arrive at this conclusion? We first recall the definition of multiplicity of a given species, A:

$$\text{multiplicity of A} = 2|s(\text{A})| + 1 \tag{27}$$

where s(A) is the total spin angular momentum quantum number of species A. Note that the absolute value of s(A) is used. Since we are dealing with a chemical reaction, this implies that we are referring to the electrons in species A and s(A) is given by

$$s(\text{A}) = \sum_{i=1}^{n} s(i) \tag{28}$$

where $s(i)$ is the spin angular momentum quantum number for the ith electron, $\pm 1/2$ (alpha spin = +1/2, beta spin = −1/2). The sum is taken from $i = 1$ to $i = n$ where n is the total number of electrons in A. For example, if A has all its molecular orbitals doubly occupied (an even number of electrons), then $|s(\text{A})| = 0$; hence the multiplicity of A is 1, which is designated as a singlet. If A is an odd electron species, with only one of its molecular orbitals singly occupied (either alpha or beta spin), then $|s(\text{A})| = 1/2$ and the multiplicity of A is 2, which is designated as a doublet. If A has two singly occupied molecular orbitals, both alpha or both beta spins, then $|s(\text{A})| = 1$ and the multiplicity of A is 3, which is designated as a triplet. Now, given a reaction A + B → C, the total number of spin states of C is given by

$$\text{total number of spin states} = (2|s(\text{A})| + 1)(2|s(\text{B})| + 1) \tag{29}$$

If we have n species in a reaction, $X_1 + X_2 + \ldots + X_n \rightarrow C$, then the total number of spin states of C is then given by

$$\prod_{j=1}^{n} 2\left|s\left(X_j\right)\right| + 1 = \left(2\left|s\left(X_1\right)\right| + 1\right)\left(2\left|s\left(X_2\right)\right| + 1\right)\ldots\left(2\left|s\left(X_n\right)\right| + 1\right) \tag{30}$$

Returning to our original example, if A and B are triplets, s(A) = ±1 and s(B) = ±1, then the total number of spin states is $(2(1) + 1)(2(1) + 1) = 9$. This answers the first part of the problem. To evaluate s(C) we use the additivity of spin angular momentum rule, sometimes referred to as Wigner's spin rule (9). The possible values of s(C) for the reaction A + B → C with known values of s(A) and s(B) is given by

$$s(\text{C}) = |s(\text{A})| + |s(\text{B})|, |s(\text{A})| + |s(\text{B})| - 1, |s(\text{A})| + |s(\text{B})| - 2, \ldots, |s(\text{A}) - s(\text{B})| \tag{31}$$

The maximum value s(C) can have is $|s(\text{A})| + |s(\text{B})|$ and the minimum value is $|s(\text{A}) - s(\text{B})|$. Again, going back to our example, if s(A) = ±1 and s(B) = ±1, then s(C) = {2, 1, 0}. This means that C can be a quintet, a triplet, or a singlet.

The final determination is the probability distribution. To obtain this, we write the values of the total magnetic spin angular momentum quantum numbers for C, m(C). Recall that the total magnetic spin angular momentum quantum number, m, is related to the total spin angular momentum quantum number, s, in the following way

$$m = s, s - 1, s - 2, \ldots, -s \tag{32}$$

Taking each case in turn, we have

$$\begin{aligned} &s(\text{C}) = 0, m(\text{C}) = 0 && \text{1 singlet state} \\ &s(\text{C}) = 1, m(\text{C}) = \{1, 0, -1\} && \text{3 triplet states} \\ &s(\text{C}) = 2, m(\text{C}) = \{2, 1, 0, -1, -2\} && \text{5 quintet states} \end{aligned} \tag{33}$$

Note that the total number of spin states is 1 + 3 + 5 = 9 as we found before. The corresponding probabilities are then 1/9 singlet, 3/9 = 1/3 triplet, and 5/9 quintet. One can continue the analysis for the following cases for the reaction A + B → C and verify that

1. If A and B are singlets, then C can only be a singlet.
2. If A is a singlet and B is a triplet, then C can only be a triplet.
3. If A and B are doublets (for example, radical species), then C can be a singlet with 1/4 probability or a triplet with 3/4 probability.
4. If A is a doublet and B is a triplet, then C can be a doublet with 1/3 probability or a quartet with 2/3 probability.
5. If *A* is a doublet and *B* is a singlet, then *C* can only be a doublet.

Having understood the problem for a bimolecular reaction, it is possible to apply the same methodology to termolecular reactions, although these would occur much less frequently in reaction mechanisms for solution-phase photochemical reactions. Hence for the reaction A + B + C → D where, suppose, A is a singlet, B is a doublet, and C is a triplet, we can ask what are the allowed multiplicities of D. Firstly, we have

$$\left|s\left(\text{A}\right)\right| = 0; \quad \left|s\left(\text{B}\right)\right| = \frac{1}{2}; \quad \left|s\left(\text{C}\right)\right| = 1 \tag{34}$$

and the total number of spin states for D is 6 (using eq 30). We apply Wigner's rule in succession, first to A and B and then to C, using E as our "intermediate" species.

$$\text{A} + \text{B} \rightarrow \text{E}$$

$$\text{E} + \text{C} \rightarrow \text{D}$$

It can be shown that the same result is obtained if B and C are chosen first and then A. Using eqs 31 and 32 we have,

$$s(\mathrm{E}) = \frac{1}{2}$$
$$s(\mathrm{D}) = \left\{\frac{3}{2}, \frac{1}{2}\right\} \qquad (35)$$
$$s(\mathrm{D}) = \frac{3}{2}, m(\mathrm{D}) = \left\{\frac{3}{2}, \frac{1}{2}, -\frac{1}{2}, -\frac{3}{2}\right\} \quad 4 \text{ quartet states}$$
$$s(\mathrm{D}) = \frac{1}{2}, m(\mathrm{D}) = \left\{\frac{1}{2}, -\frac{1}{2}\right\} \quad 2 \text{ doublet states}$$

and that the probability distribution for the multiplicity of D is 2/3 quartet and 1/3 doublet.

Summary

Four problems from various areas in physical organic chemistry have been analyzed with the aid of mathematical techniques and a clearer understanding of them has been achieved. Mathematical concepts provide a useful and powerful resource for gaining new insights in the solution of important problems in chemistry.

Acknowledgments

I would like to thank those teachers who have sparked my interest in physical organic chemistry at the University of Toronto, where I did my graduate work, especially Jerry Kresge, Tom Tidwell, John Bunting, and Keith Yates. I would also like to thank Dean Weldon and Tito Scaiano at the University of Ottawa for sparking my curiosity in analyzing problems 3 and 4, respectively. And finally, I would like to thank Graham McFarlane and my fellow colleagues at The University of Queensland for helpful contributions and discussions during the preparation of this manuscript.

Literature Cited

1. Silverstein, R. M.; Bassler, G. C.; Morrill, T. C. *Spectrometric Identification of Organic Compounds*, 4th ed.; Wiley: New York, 1981; p 35. Rose, M. E.; Johnstone, R. A. W. *Mass Spectrometry for Chemists and Biochemists*; University Press: Cambridge, 1982.
2. Lowry, T. H.; Richardson, K. S. *Mechanism and Theory in Organic Chemistry*; Harper & Row: New York, 1981. Isaacs, N. S. *Physical Organic Chemistry*; Wiley: New York, 1987.
3. Turro, N. J. *Modern Molecular Photochemistry*; University Science Books: Mill Valley, CA, 1991.
4. (a) Marcus, R. A. *J. Phys. Chem.* 1968, *72*, 891–899. (b) Kresge, A. J. *Chem. Soc. Rev.* 1973, *4*, 475–503. (c) Koeppl, G. W.; Kresge, A. J. *J. Chem. Soc. Chem. Commun.* 1973, 371–373.
5. Beynon, J. H. *Mass Spectrometry and Its Applications to Organic Chemistry*; Elsevier: Amsterdam, 1960; Chapter 8. Beynon, J. H.; Williams, A. E. *Mass and Abundance Tables for Use in Mass Spectrometry*; Elsevier: Amsterdam, 1963. Beynon, J. H.; Saunders, R. A.; Williams, A. E. *The Mass Spectra of Organic Molecules*; Elsevier: Amsterdam, 1968.
6. Burington, R. S. *Handbook of Mathematical Tables and Formulas*, 4th ed.; McGraw-Hill: New York, 1965; p 4.
7. Harris, R. K. *Nuclear Magnetic Resonance Spectroscopy: A Physicochemical View*; Pitman: London, 1983; Chapter 2.
8. Closs, G. L.; Calcaterra, L. T.; Green, N. J.; Penfield, K. W.; Miller, J. R. *J. Phys. Chem.* 1986, *90*, 3673–3683.
9. Levine, I. N. *Quantum Chemistry*, 3rd ed.; Allyn & Bacon: Boston, 1983; pp 268–272.
10. Lowry, T. H.; Richardson, K. S. *Mechanism and Theory in Organic Chemistry*; Harper & Row: New York, 1987.

Appendix

The evaluation of the intersection points of two general parabolas of different curvatures follows. We start with the general expressions

$$\begin{aligned}(r-p_1)^2 &= 4a_1(G_1-q_1)\\ (r-p_2)^2 &= 4a_2(G_2-q_2)\end{aligned} \qquad (A1)$$

as before with $a_1, a_2 > 0$ and $p_2 - p_1 > 0$. The condition $G_1 = G_2$ leads to

$$r_i = \frac{-B \pm \sqrt{B^2 - 4AC}}{2A} \qquad (A2)$$

where

$$\begin{aligned}A &= a_2 - a_1\\ B &= 2(a_1p_2 - p_1a_2)\\ C &= a_2p_1^2 - a_1p_2^2 - 4a_1a_2(q_2 - q_1)\end{aligned} \qquad (A3)$$

This indicates that there are two possible points of intersection. We make the further simplification that the minimum point of the initial (reactant) state parabola is at the origin (0, 0) so that $p_1 = 0$ and $q_1 = 0$. The result is that the final (product) state parabola is referenced relative to the initial (reactant) state parabola. Hence, we have

$$\begin{aligned}A &= a_2 - a_1\\ B &= 2a_1p_2\\ \mathrm{C} &= -(a_1p_2^2 + 4a_1a_2q_2)\end{aligned} \qquad (A4)$$

and

$$\Delta G^\circ = q_2 \qquad (A5)$$

We note that $0 < r_i < p_2$ because the final-state parabola is displaced horizontally to the right of the initial-state parabola along the reaction coordinate and that $B^2 - 4AC > 0$ for real-valued r_i. Also, from eq A4 the conditions $B > 0$ and $C < 0$ apply; whereas A can be positive or negative valued. The ordinates of the intersection points are given by

$$G_i = \frac{r_i^2}{4a_1} \qquad (A6)$$

and the change in free energy of activation represented geometrically by the vertical distance between the points (r_i, G_i) and (0, 0) is given by

$$\Delta G^\# = G_i \qquad (A7)$$

Substitution of the relationships in eq A4 into eq A2 and then applying eqs A6 and A7 successively yields

$$\Delta G^\# = \frac{p_2^2(a_1+a_2) + 4a_2(a_2-a_1)\Delta G^\circ \pm 2p_2\sqrt{a_1a_2\left(p_2^2 + 4\Delta G^\circ(a_2-a_1)\right)}}{4(a_2-a_1)^2} \qquad (A8)$$

This expression is similar to the one given in ref *4c* with the following substitutions

$$\begin{aligned}\Delta G^\# &= E_a; \quad \Delta G^\circ = \Delta E; \quad p_2 = d\\ a_1 &= \frac{1}{2k_1}; \quad a_2 = \frac{1}{2k_2}\end{aligned} \qquad (A9)$$

Equation A8 indicates that there are two possible values for $\Delta G^\#$ depending on the choice of sign of the square root term. To find out which value is meaningful, we reduce this complicated expression to the case of equal curvatures for the parabolas; that is, when $a_1 = a_2$. The case leading to the simplified Marcus expression (eq 19) would be the correct one. We first write eq A8 only in terms of a_1 with the substitution

$$a_2 = na_1 \qquad (A10)$$

and obtain

$$\Delta G^\# = \frac{p_2^2a_1(n+1) + 4a_1^2\Delta G^\circ n(n-1) \pm 2p_2a_1\sqrt{n\left(p_2^2 + 4a_1\Delta G^\circ(n-1)\right)}}{4(n-1)^2a_1^2} \qquad (A11)$$

so that when $n = 1$ both reactant and product state parabolas have equal curvatures. For the case of the positive root, setting $n = 1$ leads to a value of $\Delta G^{\#}$ that diverges to infinity; however for the case of the negative root, setting $n = 1$ leads to the indeterminate form 0/0, which can be resolved by applying L'Hôpital's rule. Hence,

$$\lim_{n\to 1}\frac{p_2^2 a_1(n+1)+4a_1^2\Delta G^\circ n(n-1)-2p_2a_1\sqrt{n\left(p_2^2+4a_1\Delta G^\circ(n-1)\right)}}{4(n-1)^2a_1^2}=$$
$$\frac{1}{4a_1}\left(\frac{4a_1^2(\Delta G^\circ)^2}{p_2^2}+2a_1\Delta G^\circ+\frac{p_2^2}{4}\right) \qquad \text{(A12)}$$

Making the substitution

$$\lambda=\frac{p_2^2}{4a_1} \qquad \text{(A13)}$$

in eq A12 and factoring leads to the quadratic form identical to the simple Marcus expression. Hence, for the case of parabolas of unequal curvature, the appropriate expression for $\Delta G^{\#}$ in eq A8 is the one with the negative sign before the square root term.